

DISCOVERY OF AN ENERGETIC 38.5 ms PULSAR POWERING THE GAMMA-RAY SOURCE IGR J18490–0000/HESS J1849–000

E. V. GOTTHELF¹, J. P. HALPERN¹, R. TERRIER² AND F. MATTANA²

(Received 2010 December 9; Accepted 2011 January 25)

To Appear in The Astrophysical Journal Letters

ABSTRACT

We report the discovery of a 38.5 ms X-ray pulsar in observations of the soft γ -ray source IGR J18490–0000 with the *Rossi X-ray Timing Explorer* (*RXTE*). PSR J1849–0001 is spinning down rapidly with period derivative $1.42 \times 10^{-14} \text{ s s}^{-1}$, yielding a spin-down luminosity $\dot{E} = 9.8 \times 10^{36} \text{ erg s}^{-1}$, characteristic age $\tau_c \equiv P/2\dot{P} = 42.9 \text{ kyr}$, and surface dipole magnetic field strength $B_s = 7.5 \times 10^{11} \text{ G}$. Within the *INTEGRAL*/IBIS error circle lies a point-like *XMM-Newton* and *Chandra* X-ray source that shows evidence of faint extended emission consistent with a pulsar wind nebula (PWN). The *XMM-Newton* spectrum of the point source is well fitted by an absorbed power-law model with photon index $\Gamma_{PSR} = 1.1 \pm 0.2$, $N_H = (4.3 \pm 0.6) \times 10^{22} \text{ cm}^{-2}$, and $F_{PSR}(2–10 \text{ keV}) = (3.8 \pm 0.3) \times 10^{-12} \text{ erg cm}^{-2} \text{ s}^{-1}$, while the spectral parameters of the extended emission are roughly $\Gamma_{PWN} \approx 2.1$ and $F_{PWN}(2–10 \text{ keV}) \approx 9 \times 10^{-13} \text{ erg cm}^{-2} \text{ s}^{-1}$. IGR J18490–0000 is also coincident with the compact TeV source HESS J1849–000. For an assumed distance of 7 kpc in the Scutum arm tangent region, the 0.35–10 TeV luminosity of HESS J1849–000 is 0.13% of the pulsar’s spin-down energy, while the ratio $F(0.35–10 \text{ TeV})/F_{PWN}(2–10 \text{ keV}) \approx 2$. These properties are consistent with leptonic models of TeV emission from PWNe, with PSR J1849–0001 in a stage of transition from a synchrotron X-ray source to an inverse Compton γ -ray source.

Subject headings: ISM: supernova remnants — pulsars: individual (HESS J1849–000, IGR J18490–0000, PSR J1849–0001) — stars: neutron

1. INTRODUCTION

The detection of 10^{12} eV emission associated with supernova products in the Galaxy has opened up a new window on the evolution of these energetic stellar remnants. More than 2/3 of the now > 60 Galactic TeV sources are supernova remnants or pulsar wind nebulae (PWNe), the latter being the largest class³. Many of these TeV PWNe are spatially offset from middle-aged ($\tau_c \sim 10^4 - 10^5 \text{ year old}$) pulsars, and are often more extended and more luminous than their X-ray PWNe counterparts. This TeV emission is likely to be inverse Compton scattered radiation from relic electrons produced by the pulsar in an earlier stage of energetic spin-down (de Jager & Djannati-Ataï 2008; Zhang et al. 2008; Mattana et al. 2009a). In contrast, younger ($\tau_c \sim 10^3 \text{ year old}$) pulsars are associated with compact TeV sources that are co-located with their X-ray PWNe. In these younger systems the high magnetic fields make for efficient synchrotron X-ray sources, and inefficient inverse Compton TeV emission.

HESS J1849–000 is one of the fainter sources detected in the HESS Galactic Plane survey (Aharonian et al. 2005, 2006) and subsequent dedicated observations, with significance of 6.4σ , flux $> 350 \text{ GeV}$ of $\approx 15 \text{ mCrab}$, and only weak indication of extent (Terrier et al. 2008). HESS J1849–000 is coincident in position with the

INTEGRAL/IBIS source IGR J18490–0000 that was discovered during a survey of the tangent regions of the Sagittarius and Scutum spiral arms (Molkov et al. 2004; Bird et al. 2006). Follow-up X-ray observation of IGR J18490–0000 by Rodriguez et al. (2008) with the *Swift* X-ray telescope (XRT) located a highly absorbed X-ray point source within the *INTEGRAL*/IBIS error circle. These authors suggested a Galactic X-ray binary origin for IGR J18490–0000 based on a *K*-band Two Micro All Sky Survey star located within the *Swift* XRT error circle. However, that association was excluded by the precise X-ray position obtained in a brief *Chandra* High Resolution Camera (HRC) observation (Ratti et al. 2010). Terrier et al. (2008) used imaging and spectroscopic evidence from an *XMM-Newton* observation to argue that IGR J18490–0000 is instead a pulsar/PWN. As such, it would join the dozen hard X-ray members of this class detected by *INTEGRAL*/IBIS (Mattana et al. 2009b; Renaud et al. 2010).

In Section 2 we present in detail the *XMM-Newton* imaging and spectral data that support a pulsar/PWN interpretation for IGR J18490–0000. In Section 3, we report the discovery using *Rossi X-ray Timing Explorer* (*RXTE*) of PSR J1849–0001 and its spin-down, which verifies this conjecture. In Section 4, we discuss the properties of HESS J1849–000 in the context of the spin-down parameters of PSR J1849–0001.

2. XMM-Newton OBSERVATION

An 11 ks *XMM-Newton* observation of IGR J18490–0000 (ObsID 0306170201) was acquired on 2006 April 3 using the European Photon Imaging Camera (EPIC; Turner et al. 2003). EPIC

¹ Columbia Astrophysics Laboratory, Columbia University, 550 West 120th Street, New York, NY 10027, USA; eric@astro.columbia.edu

² Astroparticule et Cosmologie, Université Paris 7/CNRS/CEA, Batiment Condorcet, 75013 Paris, France

³ VHE γ -ray Sky Map and Source Catalog,

[http://www.mppmu.mpg.de/\\$\sim\\$rwagner/sources/index.html](http://www.mppmu.mpg.de/\simrwagner/sources/index.html)

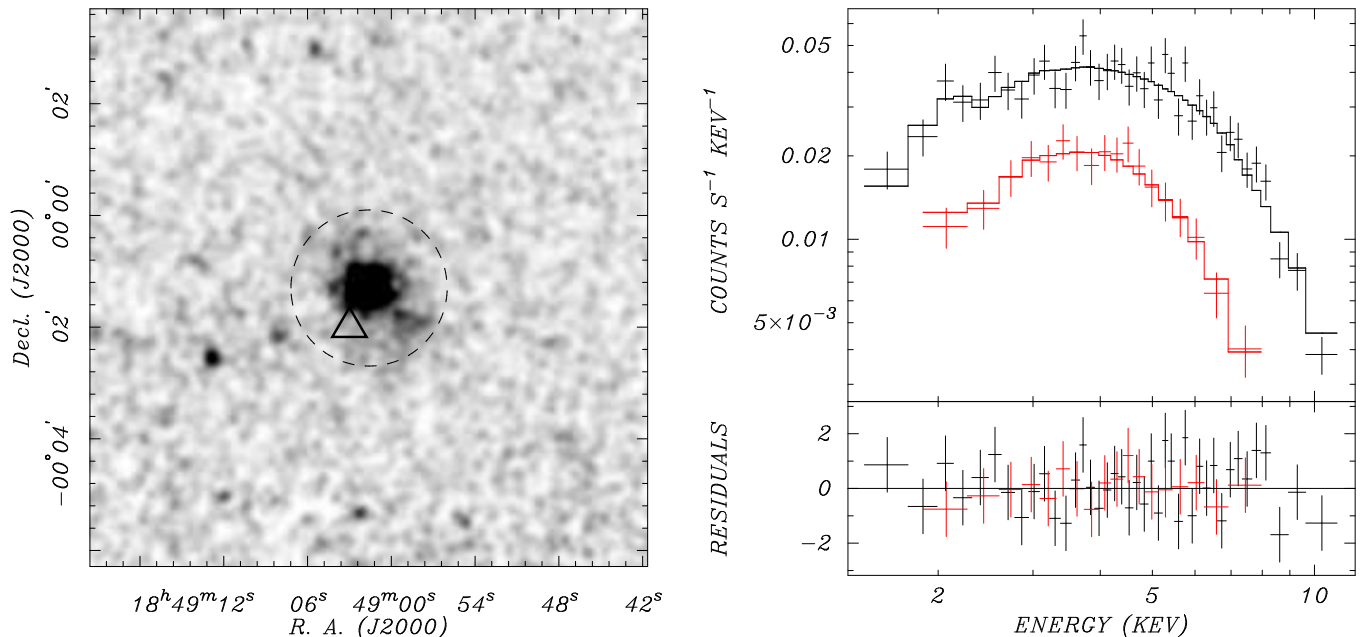


Figure 1. *XMM-Newton* EPIC X-ray observation of the *INTEGRAL*/IBIS source IGR J18490–0000. Left: exposure corrected and smoothed EPIC MOS image scaled in intensity to highlight the faint diffuse emission near the point source. This source, the putative pulsar, lies within the *INTEGRAL*/IBIS $r = 1.4$ positional uncertainty of IGR J18490–0000 (Terrier et al. 2008; dashed circle), as does the centroid of HESS J1849–000, indicated by the triangle. Right: *XMM-Newton* EPIC pn (black) and EPIC MOS (red) spectra of the point source fitted to the model described in the text. The lower panel shows residuals from the best fit in units of 1σ .

consists of three sensors operating in parallel, one pn and two MOS CCD cameras. These instruments are sensitive to X-rays in the 0.2–12 keV range with energy resolution $\Delta E/E \approx 0.1/\sqrt{E(\text{keV})}$. All three cameras were operated in full-frame mode, using the thin and medium filters for the EPIC pn and MOS, respectively. The target was placed at the default EPIC pn focal plane location for a point source. The time resolution of 73.4 ms and 2.7 s for the EPIC pn and MOS, respectively, are insufficient to search for a typical pulsar signal.

The data were processed using the SAS version xmm-sas_20061026_1802-6.6.0 pipeline, and were analyzed using both the SAS and FTOOLS software packages. The observation was free of significant particle background contamination and provided a near continuous 11 ks of good observing time for the EPIC MOS and 9.9 ks for EPIC pn.

Figure 1 (left) displays the 2–10 keV *XMM-Newton* EPIC MOS X-ray image centered on IGR J18490–0000. The image has been exposure corrected and smoothed using a $\sigma = 3''.8$ Gaussian kernel and scaled to highlight the faint diffuse emission near the central bright source at coordinates (J2000.0) R.A. = $18^{\text{h}}49^{\text{m}}01^{\text{s}}.62$, decl. = $-00^{\circ}01'17''.7$. This source, at the position of the previously detected *Swift* XRT source, lies at the center of the 1.4 radius error circle of IGR J18490–0000. There are no other prominent X-ray sources in the full $30'$ diameter field of this instrument. Together with the positional coincidence, its flux and spectrum (see below) leave no doubt that XMMU J184901.6–000117 is the counterpart of IGR J18490–0000. Faint, diffuse emission surrounds the point source, and a prominent feature extends up to $2'$ to the southwest; these properties are suggestive of a PWN. A 1.2 ks *Chandra* HRC image obtained on

2008 February 16 (Ratti et al. 2010) shows that most of the *XMM-Newton* source flux is contained in a point-like component.

2.1. *XMM-Newton* Point-source Spectrum

A spectrum of XMMU J184901.6–000117 was extracted from each EPIC camera using a $30''$ radius aperture centered on the point source; data from the two MOS cameras were combined into a single spectrum. The source background was estimated using counts from an $60''$ aperture placed just south of the source region, on the same CCD of each camera. These source spectra were grouped with a minimum of 50 counts per spectral channel and fitted using the XSPEC fitting package (Arnaud 1996). EPIC pn and MOS spectra were fitted simultaneously with a single absorbed power-law model, allowing independent flux normalization (Figure 1, right); we report the average of the fluxes measured by the two EPIC cameras. In the following, all derived luminosities are corrected for interstellar absorption, fluxes are uncorrected, and errors are at the 90% confidence level. The data yield a good fit with a reduced $\chi^2_{\nu} = 0.90$ for 72 degrees of freedom (dof). The hard spectrum has photon index $\Gamma_{\text{PSR}} = 1.1 \pm 0.2$, $N_{\text{H}} = (4.3 \pm 0.6) \times 10^{22} \text{ cm}^{-2}$, and $F_{\text{PSR}}(2-10 \text{ keV}) = (3.8 \pm 0.3) \times 10^{-12} \text{ erg cm}^{-2} \text{ s}^{-1}$. The Galactic coordinates of IGR J18490–0000, $(\ell, b) = (32.^{\circ}64, +0.^{\circ}53)$ are coincident with the tangent point of the Scutum arm. Considering this and the large fitted N_{H} , we hypothesize that IGR J18490–0000 is located at a distance of 7 kpc appropriate for the Scutum tangent region rather than residing in the nearer Sagittarius arm. Its 2–10 keV X-ray luminosity is then $L_{\text{PSR}}(2-10 \text{ keV}) = 2.8 \times 10^{34} d_7^2 \text{ erg s}^{-1}$.

We also fitted the *XMM-Newton* and *INTEGRAL*/IBIS spectra simultaneously, finding that a sim-

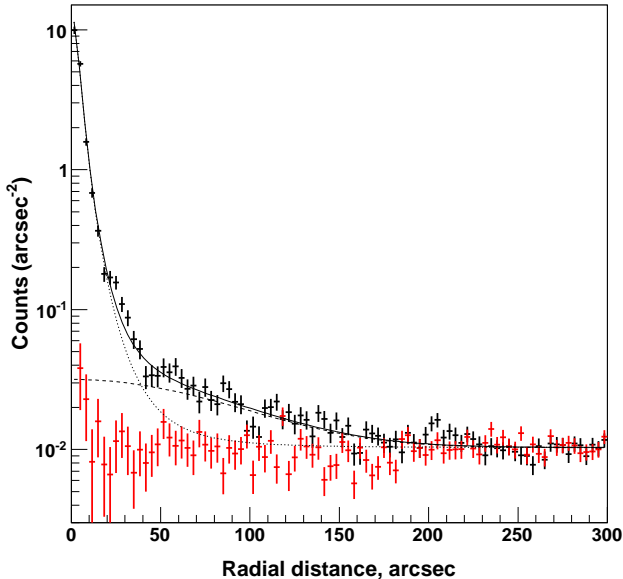


Figure 2. Radial profile of the emission from IGR J18490–0000 in the EPIC pn. The dotted line is the average King profile for a $\Gamma = 1.1$ power-law spectrum; the red points are background taken at a symmetric position with respect to the instrument optical axis. An additional extended component visible up to $150''$ from the point source is well fitted by a Gaussian profile of $\sigma = 75''$ (dashed line). The solid line is the total fitted profile.

ple power-law model gives a reasonable χ^2 but a rather poor fit to the *INTEGRAL*/IBIS data (observation and analysis of the IGR J18490–0000 data as described in Terrier et al. 2008). An excellent result is obtained by fitting a broken power law ($\chi^2_\nu = 0.95$ for 140 dof) with a break energy of 23 keV. The best fit indices of $\Gamma = 1.2 \pm 0.1$ and $\Gamma = 1.7 \pm 0.2$, for the low and high energies, respectively, are consistent with those obtained for the spectra individually (Terrier et al. 2008).

2.2. XMM-Newton Extended Emission

To quantify the spatial structure of the *XMM-Newton* source, we made a radial profile of the counts distribution centered on the point source and compared it with the point spread function (PSF). The latter was constructed using instrumental profiles at several energies weighted to match the measured spectral index. Figure 2 shows the measured EPIC pn profile compared to the average PSF for this spectrum and location in the field. Background has been taken from a symmetric position with respect to the optical axis. There is a clear excess of emission from $20''$ to $150''$ radius. We fitted the radial counts distribution to the sum of a King profile to represent the point source, and a Gaussian to represent the extended emission. A Gaussian component $150'' \pm 15''$ in diameter improves the quality of the fit by $\approx 9\sigma$, proving that the source is surrounded by a nebula or a halo.

We extracted the spectrum of the extended nebula in an annulus surrounding XMMU J184901.6–000117 from $30''$ to $150''$. To account for contamination from the wings of the bright point source, we fitted the point source and extended emission spectra simultaneously. We used separate power laws but the same N_H for both spectra. We added a constant fraction of the point-source spectrum to the diffuse emission. This fraction

was estimated from the PSF as 12% and 14% for EPIC pn and MOS, respectively, at a radius of $30''$. To account for the uncertainty in the estimate of these fractions, we varied them from 7% to 19% of the point-source flux, adding the corresponding systematic uncertainty to errors on the fitted parameters. The resulting diffuse emission spectrum has $\Gamma_{\text{PWN}} = 2.1 \pm 0.3$ and a flux of $F_{\text{PWN}}(2 - 10 \text{ keV}) = (9 \pm 2) \times 10^{-13} \text{ erg cm}^{-2} \text{ s}^{-1}$. The reduced chi-squared is $\chi^2_\nu = 0.90$ for 311 dof.

The extended nebula with a steeper spectrum suggests that IGR J18490–0000 is a pulsar/PWN system. Alternatively, given the large N_H , some of the diffuse emission could be a dust-scattered halo of the bright point source (Predehl & Schmitt 1995); however, that could not account for its asymmetric extension. We note that the nebula is rather faint, $\approx 25\%$ of the point source flux, but it is still in the range observed for PWNe (Kargaltsev & Pavlov 2008).

3. RXTE OBSERVATIONS

To search for the expected pulsar signal from IGR J18490–0000, we obtained 112.3 ks of *RXTE* observations, pointed at the *Chandra* source position, spanning 2010 November 25 – December 15. The schedule was designed to obtain a phase-connected timing solution that would measure both P and \dot{P} . The data used here were collected with the Proportional Counter Array (PCA; Jahoda et al. 1996) in the GoodXenon mode with an average of 1.75 out of the five proportional counter units (PCUs) active. In this mode, photons are time-tagged to $0.9 \mu\text{s}$ precision and have an absolute time accuracy of $< 100 \mu\text{s}$ (Rots et al. 1998). The effective area of five combined detectors is $\approx 6500 \text{ cm}^2$ at 10 keV with a roughly circular field of view of $\sim 1^\circ$ FWHM. Spectral information is available in the 2–60 keV energy band with a resolution of $\sim 16\%$ at 6 keV.

Standard time filtering was applied to the PCA production data, rejecting intervals of South Atlantic Anomaly passage, Earth occultation, and other periods of high particle activity. The photon arrival times were transformed to the solar system barycenter in Barycentric Dynamical Time (TDB) using the JPL DE200 ephemeris and the coordinates given in Table 1, obtained from *Chandra* HRC observation ObsID 7398. These coordinates are derived from a centroid calculation of 17 photons within a $2''$ radius aperture and have nominal uncertainty of $0''.6$. We note that these coordinates differ by $0''.35$ from those reported in Ratti et al. (2010).

3.1. RXTE Timing Analysis

We restricted the analysis to the 2 – 20 keV energy range (PCA channels 2 – 50) from the top Xenon layer of each PCU to optimize the signal-to-noise. A fast Fourier transform of the initial data set (ObsID 95309-01-01-02; 7 ks) revealed a highly significant signal of period $P = 38.52 \text{ ms}$. Subsequently, for each satellite orbit we extracted a pulse profile corresponding to the peak power as determined by the Rayleigh test (Strutt 1880), also known as Z_1^2 (Buccheri et al. 1983). The resulting profiles were cross-correlated, shifted, and summed to generate a master pulse profile template. Each individual profile was then cross correlated with this template to determine its time of arrival (TOA) and uncertainty.

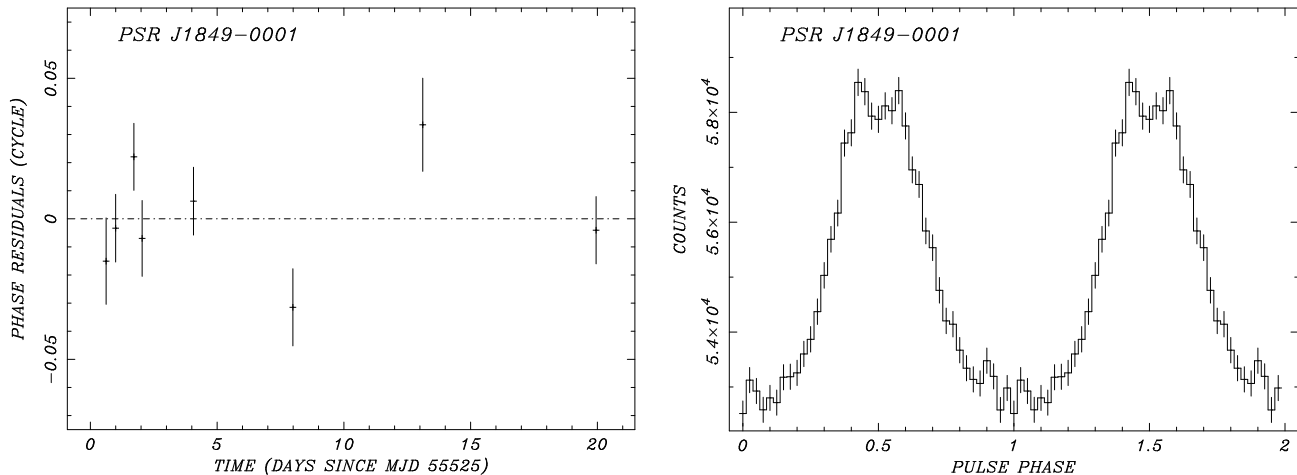


Figure 3. Discovery timing results for the X-ray pulsar PSR J1849-0001 using *RXTE* data. Pulse phase residuals (left) and folded light curve (right) of PSR J1849-0001 in the 2–20 keV band were generated using the quadratic ephemeris of Table 1. Phase zero of the light curve corresponds to the ephemeris epoch; two cycles are shown for clarity.

Table 1
Timing Parameters of PSR J1849-0001

Parameter	Value
R.A. (J2000.0) ^a	18 ^h 49 ^m 01. ^s 61
Decl. (J2000.0) ^a	−00°01′17″6
Epoch (MJD TDB)	55535.285052933
Period ^b , P	38.518943432(12) ms
Period derivative ^b , \dot{P}	$1.4224(58) \times 10^{-14} \text{ s s}^{-1}$
Range of dates (MJD)	55525.6 – 55545.2
Spin-down luminosity, \dot{E}	$9.8 \times 10^{36} \text{ erg s}^{-1}$
Characteristic age, τ_c	42.9 kyr
Surface dipole magnetic field, B_s	$7.5 \times 10^{11} \text{ G}$

^a *Chandra* position with a nominal uncertainty of 0″.6 (see the text).

^b TEMPO 1 σ uncertainties given in parentheses.

These TOAs were then iteratively fitted to a quadratic ephemeris.

The resulting unique ephemeris is presented in Table 1, and the phase residuals are shown in Figure 3. The residuals are all less than 0.05 cycles and do not require a higher derivative. The derived properties of PSR J1849-0001 are: spin-down luminosity $\dot{E} = 4\pi^2 I \dot{P} / P^3 = 9.8 \times 10^{36} \text{ erg s}^{-1}$, characteristic age $\tau_c \equiv P / 2\dot{P} = 42.9 \text{ kyr}$, and surface dipole magnetic field strength $B_s = 3.2 \times 10^{19} (P\dot{P})^{1/2} = 7.5 \times 10^{11} \text{ G}$.

Figure 3 displays the summed pulse profile using all the 2–20 keV data folded on the final ephemeris. It has a symmetric, single-peaked structure. The raw pulsed fraction is 3.8%, uncorrected for PCA instrument or astrophysical background, difficult to determine with sufficient accuracy for this purposes. We see no energy dependence of the pulse profile when subdividing the 2–20 keV band.

3.2. *RXTE* Spectral Analysis

The spectrum of the pulsed flux from PSR J1849-0001 can be isolated by phase-resolved spectroscopy. We used the *fasebin* software to construct phase-dependent spectra based on the ephemeris of Table 1. For each ObsID and PCU we constructed spectra from counts detected in the top Xenon layer only and combined them to produce a single spectrum per PCU for the entire set of observa-

tions. Similarly, standard PCA responses for each PCU were generated at each ObsID and averaged. In fitting the pulsed flux, the unpulsed emission provides a near perfect background estimate and was taken from the 0.4 phase bins range corresponding to the region of flat minimum in the pulse profile around phase zero.

The merged *RXTE* spectrum was fitted in the 2 – 20 keV range using a simple absorbed power-law model with the interstellar absorption held fixed at $N_H = 4.3 \times 10^{22} \text{ cm}^{-2}$ determined from the *XMM-Newton* fit (see Figure 4). The resulting best-fit photon index is $\Gamma = 1.3^{+0.2}_{-0.3}$. The 2–10 keV pulsed flux is $8.9 \times 10^{-13} \text{ erg cm}^{-2} \text{ s}^{-1}$, which represents $\sim 25\%$ of the point-source flux of PSR J1849-0001 measured by *XMM-Newton*. The corresponding pulsed luminosity (assumed isotropic) is $6.7 \times 10^{33} d_7^2 \text{ erg s}^{-1}$. The reduced chi-squared is $\chi^2_\nu = 0.70$ for 29 dof.

As expected, the *RXTE* measured spectral slope is intermediate between the *XMM-Newton* and *INTEGRAL*/IBIS values, indicating a steepening around 10 – 20 keV.

4. DISCUSSION AND CONCLUSIONS

The discovery of PSR J1849-0001 using *RXTE* verifies the conjecture of Terrier et al. (2008) that XMMU J184901.6-000117, IGR J18490-0000, and HESS J1849-000 are all manifestations of a young pulsar/PWN system. Even though the *RXTE* field of view is wider than those of *XMM-Newton* and *Chandra*, there is little doubt that PSR J1849-0001 is the compact source in IGR J18490-0000, given the morphological and spectral evidence, and the compatibility of the *RXTE* measured pulsed flux with that of XMMU J184901.6-000117. Terrier et al. (2008) estimated that the spin-down luminosity of PSR J1849-0001 would be $\approx 9 \times 10^{36} \text{ erg s}^{-1}$ based on the empirical correlation between \dot{E} and Γ_{PSR} of Gotthelf (2003); this turns out to have been an accurate prediction.

Assuming a distance of 7 kpc as proposed in Section 2.1, the X-ray luminosities of the pulsar and PWN, $L_{\text{PSR}}(2 - 10 \text{ keV}) = 2.9 \times 10^{-3} \dot{E} d_7^2$ and $L_{\text{PWN}}(2 - 10 \text{ keV}) = 6.6 \times 10^{-4} \dot{E} d_7^2$, respectively,

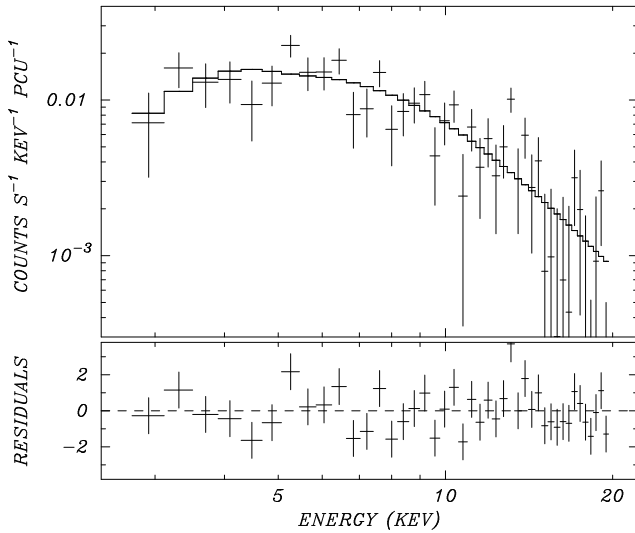


Figure 4. *RXTE* spectrum of pulsed flux from PSR J1849–0001 obtained by subtracting the off-peak spectrum from the on-peak spectrum, and fitting to an absorbed power-law model (see the text).

are consistent with the range of pulsar/PWN systems (Kargaltsev & Pavlov 2008). The 20 – 100 keV flux of IGR J18490–0000 measured by *INTEGRAL*/IBIS (2×10^{-11} erg cm $^{-2}$ s $^{-1}$; Terrier et al. 2008) corresponds to $L(20 - 100 \text{ keV}) = 0.012 \dot{E} d_7^2$. Given the 2 – 20 keV flux and spectral information from *XMM-Newton* and *RXTE*, the *INTEGRAL*/IBIS source is likely to be dominated by the pulsar rather than the PWN.

The TeV flux from HESS J1849–000 (2.2×10^{-12} erg cm $^{-2}$ s $^{-1}$; Terrier et al. 2008) corresponds to $L(0.35 - 10 \text{ TeV}) = 1.3 \times 10^{-3} \dot{E} d_7^2$. Such a small efficiency of converting spin-down power to high-energy radiation is typical of high \dot{E} pulsars. The ratio $F(0.35 - 10 \text{ TeV})/F_{\text{PWN}}(2 - 10 \text{ keV}) \approx 2$ falls squarely on the inverse correlation between this quantity and \dot{E} that was fitted by Mattana et al. (2009a), and modeled by them in terms of an evolving PWN emitting synchrotron X-rays and inverse Compton γ -rays. PSR J1849–0001 is in transition from a synchrotron dominated X-ray PWN to

an inverse Compton scattered TeV nebula, an expected phase through which a middle-aged pulsar will pass.

We thank the *RXTE* project for making the time available for this program, and the mission planners for carefully scheduling the observations. This investigation is also based on observations obtained with *XMM-Newton*, an ESA science mission with instruments and contributions directly funded by ESA Member States, and NASA.

REFERENCES

- Aharonian, F., et al. 2005, *Science*, 307, 1938
 Aharonian, F., et al. 2006, *ApJ*, 636, 777
 Arnaud, K. A., 1996, in ASP Conf. Ser. 101, *Astronomical Data Analysis Software and Systems V*, eds. G. Jacoby and J. Barnes (San Francisco, CA: ASP), p17
 Bird, A. J., et al. 2006, *ApJ*, 636, 765
 Buccheri, R., et al. 1983, *A&A*, 128, 245
 de Jager, O. C., & Djannati-Ataï, A. 2008, in *Astrophysics and Space Science 357, Neutron Stars and Pulsars*, ed. W. Becker (Berlin: Springer), 451
 Gotthelf, E. V. 2003, *ApJ*, 591, 361
 Jahoda, K., Swank, J. H., Giles, A. B., Stark, M. J., Strohmayer, T., Zhang, W., & Morgan, E. H. 1996, *Proc. SPIE*, 2808, 59
 Kargaltsev, O., & Pavlov, G. G. 2008, in *AIP Conf. Proc. 983, 40 Years of Pulsars: Millisecond Pulsars, Magnetars, and More*, ed. C. Basa et al. (Melville, NY: AIP), 171
 Mattana, F., Götz, D., Terrier, R., Renaud, M., & Falanga, M. 2009b, in *AIP Conf. Proc. 1126, Simbol-X: Focusing on the Hard X-ray Universe*, ed. J. Rodriguez, & P. Forrondo (Melville, NY: AIP), 259
 Mattana, F., et al. 2009a, *ApJ*, 694, 12
 Molkov, S. V., Cherepashchuk, A. M., Lutovinov, A. A., Revnivtsev, M. G., Postnov, K. A., & Sunyaev, R. A. 2004, *Astron. Lett.*, 30, 534
 Predehl, P., & Schmitt, J. H. M. M. 1995, *A&A*, 293, 889
 Ratti, E. M., Bassa, C. G., Torres, M. A. P., Kuiper, L., Miller-Jones, J. C. A., & Jonker, P. G. 2010, *MNRAS*, 408, 1866
 Renaud, M., et al. 2010, *ApJ*, 716, 663
 Rodriguez, J., Tomsick, J. A., & Chaty, S. 2008, *ApJ*, 482, 731
 Rots, A. H., et al. 1998, *ApJ*, 501, 749
 Strutt, J. W. 1880, *Phil. Mag.*, 10, 73
 Terrier, R., Mattana, F., Djannati-Ataï, A., Marandon, V., Renaud, M., & Dubois, F. 2008, in *AIP Conf. Proc. 1085, High Energy Gamma-ray Astronomy*, ed. F. A. Aharonian, W. Hofmann, & F. Rieger (Melville, NY: AIP), 312
 Turner, M. J. L., Briel, U. G., Ferrando, P., Griffiths, R. G., & Villa, G. E. 2003, *Proc. SPIE*, 4851, 169
 Zhang, L., Chen, S. B., & Fang, J. 2008, *ApJ*, 676, 1210